



Development of self-stressing Engineered Cementitious Composites (ECC)

He Zhu^a, Duo Zhang^a, Yichao Wang^{a,b}, Tianyu Wang^{a,c}, Victor C. Li^{a,*}

^a Department of Civil and Environmental Engineering, University of Michigan, Ann Arbor, MI, 48109, USA

^b Department of Disaster Mitigation for Structures, College of Civil Engineering, Tongji University, Shanghai, 200092, China

^c College of Engineering, China University of Geosciences-Wuhan, Wuhan, Hubei Province, 430074, China

ARTICLE INFO

Keywords:

Engineered cementitious composites (ECC)
Calcium sulphoaluminate cement (CSA)
Shrinkage reducing agent (SRA)
Shrinkage
Expansion
Self-stressing
Polypropylene (PP) fiber

ABSTRACT

While high ductility Engineered Cementitious Composites (ECC) have demonstrated effectiveness for infrastructure repair, the microcracking induced by the high material shrinkage may decrease the structural durability of ECC in aggressive environments. The objective of this research is to develop a self-stressing ECC, the expansion of which against the restraint of the repaired structure automatically induces pressure onto the repair material. Super absorbent polymer (SAP), shrinkage reducing agent (SRA), and calcium sulphoaluminate cement/expansive additive (CSA) were utilized together with Portland cement to tailor the composite expansion and expansive pressure. Free drying expansion/shrinkage, restrained expansive stress, and tensile performance were examined through standard shrinkage measurement, steel ring restraint test, and uniaxial tensile test, respectively. It was found that the 28 days drying shrinkage was decreased by 47% due to the use of SRA but was slightly increased when SAP was used. Substituting 42% of OPC with CSA (K42) increased ECC strength and ductility. The K42-ECC experienced a maximum expansion of 3756 μe at 3 days and retained 2026 μe expansion at 28 days. However, the expansion loss between 3 days and 28 days counteracted the expansive pressure. The deliberate combination of SRA and CSA provides a self-stressing effect tailoring the maximum expansion and expansion loss. The self-stressing performance along with a 7% ultra-high strain capacity and average crack width of 35–44 μm at 3% strain promotes the developed ECC as a more durable material for infrastructure repair.

1. Introduction

Due to the brittle nature of concrete, aging infrastructures face the challenge of cracking and excessive deterioration. According to the ASCE infrastructure report card (2017) [1], US civil infrastructure received a Grade of D, indicating an urgent need for rehabilitation to maintain the desired performance and service life.

Conventional cementitious materials are brittle, with a low tensile strain capacity of approximate 0.01%. To attain high strength and dense microstructure, repair cementitious materials are usually designed with a large quantity of fine reactive powders at low water content. This combination results in a high shrinkage of the cementitious material [2], which can lead to restrained shrinkage cracking [3]. After cracking, the external fluid containing harmful species may ingress through the cracks leading to steel corrosion and further deteriorations of the concrete element.

To overcome the inherent brittleness of cementitious materials, Engineered Cementitious Composites (ECC) has been developed and

adopted for repair applications [4–6]. Typical ECC exhibits high tensile strain capacity (>3%) and intrinsically tight crack width (<100 μm) [5]. The high ductility of ECC is realized by the formation of multiple fine cracks in place of a single wide crack typically found in conventional concrete. However, ECC is generally made with high volumes of cementitious materials and fine aggregate with no coarse aggregate, resulting in a high drying shrinkage up to –1500 μe at 28 days [7]. Though ECC will not fail under the restrained drying shrinkage due to its tensile strain-hardening response, the presence of microcracks in an aggressive environment may lower the durability of the repair [8].

Concrete shrinkage can be reduced by incorporating superabsorbent polymer (SAP) and shrinkage reducing agent (SRA). SAP was demonstrated to reduce the autogenous shrinkage [9] in high strength concrete by providing extra internal water during curing. However, the effectiveness of using SAP for shrinkage reduction remains open for question, since both positive [10] and negative effects [11] on drying shrinkage have been observed in SAP concrete. SRA was reported to reduce drying shrinkage by up to 68.7% by reducing the surface tension of the fluid in

* Corresponding author.

E-mail addresses: zhuhe14@tsinghua.org.cn, zhuhe@umich.edu (H. Zhu), duzhang@umich.edu (D. Zhang), yicwang@umich.edu (Y. Wang), tiawang@umich.edu (T. Wang), vcli@umich.edu (V.C. Li).

<https://doi.org/10.1016/j.cemconcomp.2021.103936>

Received 22 April 2020; Received in revised form 5 November 2020; Accepted 4 January 2021

Available online 11 January 2021

0958-9465/© 2021 Elsevier Ltd. All rights reserved.

the pore system [12,13]. Increasing the dosage of SRA could further decrease concrete shrinkage but was found to reduce compressive, tensile, and flexural strength [13–15]. Despite the previous success of using SAP and SRA in ECC [2], the shrinkage magnitude of ECC remains larger than ordinary concrete.

Employing an expansive agent or expansive cement was an alternative method to mitigate concrete/ECC shrinkage. Zhang [16] developed a low shrinkage ECC with drying shrinkage of -109 to $-242 \mu\text{e}$ and tensile strain capacity of 2.5% at 28 d. The low shrinkage cement adopted by Zhang [16] was a blended composite of ordinary Portland cement (OPC) and calcium sulphoaluminate cement (CSA). By adjusting the mass ratio of CSA to OPC, both low shrinkage and expansion effects could be obtained [17,18]. Expansive cement enhances the volume stability of concrete and can even lead to the expansion of concrete [19].

By replacing OPC with CSA, the expansion increases first and subsequently decreases after reaching a peak [20,21]. In concrete repair, excessive expansion can damage the existing concrete while too little expansion is insufficient for compensating the shrinkage of the new repair material. The repair material can be tailored to exert pressure on the repaired structure by having a controlled magnitude of the expansion. The back-pressure caused by the restraining effect of the repaired structure then leads to the self-stressing of the repair material [22,23]. Cementitious materials have low elastic modulus and prominent creep at early age, so that the actual expansive stress achieved may be moderate [24]. When combined with increasing stiffness and decreasing creep with time, the reversal of expansion (expansion loss) at later age could generate tensile stress that counteracts the expansion effect at early age. This could lead to the elimination of the desired expansive pressure between the material and repaired structure. Therefore, both the maximum expansion and the subsequent expansion loss require carefully tuning to attain a self-stressing repair material.

The partial replacement of OPC by expansive cement potentially affects the mechanical performance of repair materials. Hu [25] reported the microstructure of expansive cement paste as loose with many cracks, which was improved under confined curing conditions. As a result, the tensile strain capacity of expansive mortar and concrete was increased [26]. Contradictory findings of the CSA effect on ECC has been reported in the literature. CSA was reported to reduce the tensile strength and strain capacity when utilized in ECC [13]. The decreased ductility was attributed to a high chemical bond between the CAS-modified matrix and Polyvinyl Alcohol (PVA) fiber [27]. However, no adverse effect on ductility was found in another study [20]. Polypropylene (PP) fiber revealed a different bonding performance with CSA cement [27]. ECC reinforced with PP fiber shows a promising strain capacity performance. While the above-referenced studies hint at the potential of self-stressing in ECC, its systematic development is all but missing.

The objective of this work is to develop a self-stressing ECC, which autogenously exerts pressure onto the repaired structure while maintaining an ultra-high tensile strain capacity. The restraint of the repaired structure effectively places a compressive load onto the repair material—the self-stress. SAP, SRA, CSA with different CaSO_4 contents were utilized to tailor the maximum expansion and the expansion loss. Free drying expansion/shrinkage, restrained stress, and tensile performance were examined by ECC length measurement, expansion steel ring test, and uniaxial tension, respectively.

2. Experimental program

2.1. Materials and mix proportions

Type I ordinary Portland cement (OPC, Lafarge Holcim Cement Co., MI, USA) was used. The CSA expansive additive/cement was provided by CTS Cement Manufacturing Corp. (CSA-K) and ROYAL WHITE CEMENT Inc (CSA-R), of which the CSA-R is a pure calcium sulphoaluminate clinker while CSA-K incorporates calcium sulfate. Fly ash with

a size distribution from 10 to 100 μm was provided by Boral Material Technologies Inc. The anhydride used for adjusting the expansion magnitude was obtained from USG SNOW WHITE. The chemical compositions of the cementitious materials are listed in Table 1.

The dosage of PP fiber (Table 2) was 2% volume fraction of the total composition. The 12 μm diameter, 10 mm length PP fiber Brasilit (from Saint-Gobain Brazil) has 6 GPa Young's modulus and 850 MPa tensile strength. Superplasticizer (WR, MasterGlenium 7920, BASF) was adopted as a high range water reducer, while 0.1% weight binder of Hydroxypropyl Methylcellulose (HPMC from Alfa Aesar, viscosity 7500–14000 mPa s) was used as a viscosity modifying admixture. HPMC was utilized for promoting the dispersion of PP fibers [28].

To develop the self-stressing ECC, three strategies were adopted for designing the mixtures (Table 2), including the low shrinkage method, expansive method, and a combination of both. K0 following the classic M45 binder (FA/OPC = 2.2) [29] was selected as a reference mixture. The internal curing with SAP (Sanyo Corporation, AQUA KEEP CA180 N) and shrinkage reduce admixture (SRA, GCP Applied Technologies, ECLIPSE 4500) were designed as low shrinkage strategy, named as SAP-K0 and SRA-K0. 0.4% weight binder of SAP was pre-soaked with water, which was 25 times the weight of SAP [30]. The SRA was added at 2% by binder mass as proposed by previous studies [31,32].

Regarding the expansive method, CSA-K (a blend of CSA clinker and calcium sulfate) was adopted to replace 22%, 32%, 42%, and 52% weight ratio of OPC, and the mixture ID was designated as K22, K32, K42, and K52. The pure CSA clinker (CSA-R) with 0%, 10%, 20%, and 30% replacement ratio of anhydride was employed to study the effect of CaSO_4 addition on ECC expansion, which was named as R42-A0, A10, A20, and A30. The total weight of CSA-R and anhydride were maintained 42% weight of the total cement.

Finally, the combination of SRA and CSA was studied to obtain the self-stressing ECC via both expansion and low shrinkage methods.

2.2. Test methods

2.2.1. Sample preparations

The ECC sample preparation procedure is illustrated in Fig. 1, following the sequence of pre-mix dry ingredients, add liquid, and add fibers. A 5.7 L planetary mixer was used to prepare the samples of free deformation tests (1 L/batch) and compressive and uniaxial tensile tests (1.2 L/batch). 10 L/batch of ECC was prepared with a 28.4 L planetary Hobart mixer for steel ring test. Due to the superior flowability of fresh ECC, no vibration was applied to the samples. After demolding, the samples were cured in air ($20 \pm 3^\circ\text{C}$ and $40 \pm 5\%$ RH). The details of the mold dimension and demolding time are introduced in the following sections.

2.2.2. Free shrinkage/expansion

The specimens for measuring free shrinkage/expansion were cast using a 25 by 25 by 300-mm prism mold. The drying shrinkage/expansion evolves rapidly at early age. Since restrained deformation induces restrained stress after final setting [47], the final setting time for each mixture was selected as the “zero time, t_0 ” in order to compare the drying shrinkage of different mixtures. The setting time was also the earliest time for demolding. Table 4 lists the t_0 of each mixture per ASTM C403/C403M–16 [48]. The length measurement starts immediately

Table 1

Chemical compositions determined by X-ray fluorescence of OPC, CSA, and fly ash (%).

Material	CaO	Al_2O_3	SiO_2	Fe_2O_3	MgO	SO_3
OPC	63.5	4.8	19.6	2.9	2.2	2.6
CSA-K	47.2	10.1	7.0	0.7	1.1	33.1
CSA-R	41.8	29.5	5.8	2.1	0.6	18.6
FA	17.4	19.8	39.4	11	3.70	1.9

Table 2
Mix proportion of ECC matrix (kg/m³).

Mixture	OPC	CSA-K	CSA-R	Anhydrite	FA	HPMC	Water	SRA	WR	SAP
K0	490				1077	1.5	470		1.5	
SAP-K0	490				1077	1.5	470 ^a		2.7	6.3
SRA-K0	490				1077	1.5	439	31	1.5	
K22	380	110			1077	1.5	470		1.5	
K32	333	157			1077	1.5	470		1.5	
K42	284	206			1077	1.5	470		1.5	
K52	235	255			1077	1.5	470		1.5	
R42-A0	286		206	0	1077	1.5	470		1.5	
R42-A10	286		185	21	1077	1.5	470		1.5	
R42-A20	286		165	41	1077	1.5	470		1.5	
R42-A30	286		144	62	1077	1.5	470		1.5	
SRA-K32	333	157			1077	1.5	439	31	1.5	
SRA-K42	284	206			1077	1.5	439	31	1.5	

^a The water included two-part: 157 kg/m³ for pre-soaking SAP and 313 kg/m³ for mixing.

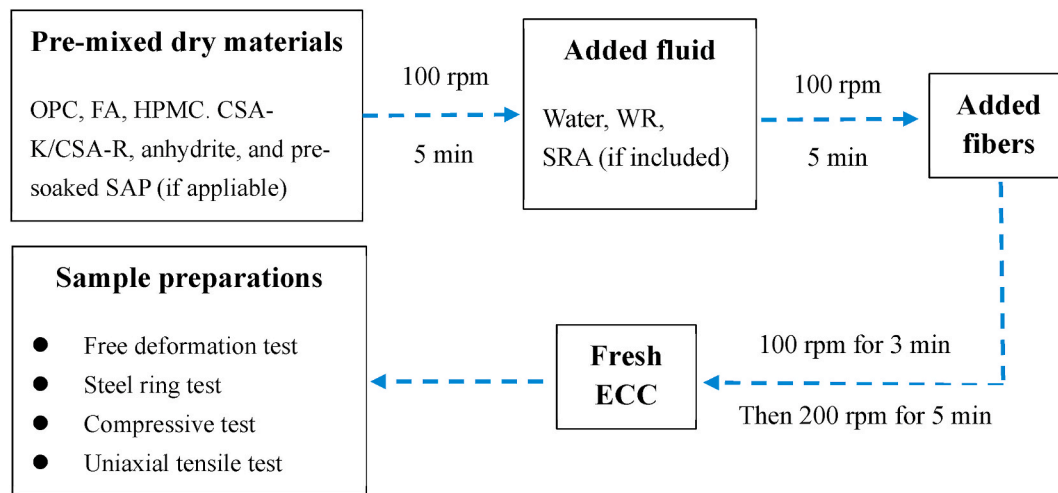


Fig. 1. The mixing procedure of ECC.

Table 3
Test protocol of the mixtures.

Mixture	Free shrinkage/ expansion	Expansion steel ring	Tension	Compression
K0	X		X	X
SAP-K0	X			
K22	X			
K32	X			
K42	X	X	X	X
K52	X			
R42-A0	X			
R42-A10	X			
R42-A20	X			
R42-A30	X			
R42-A40	X			
SRA-K0	X		X	X
SRA-K32	X			
SRA-K42	X	X	X	X

after specimen demolding until 150 days. Fig. 2 shows the length change test of the specimens according to ASTM C490/C490M-17 [33].

2.2.3. Expansion steel ring test

In order to evaluate the self-stressing property, an expansion steel

Table 4
Characteristic expansion of the ECC mixtures tested.

Mixture	t ₀ (h)	Maximum expansion		Expansion at		Expansion loss at	
		Age (d)	Expansion (µε)	28d (µε)	150d (µε)	28d (µε)	150d (µε)
K0	20	2.3	-22	-1435	-2088	1413	2066
K22	10	2.3	779	-832	-1532	1611	2311
K32	5	2.9	2418	1139	251	1279	2167
K42	5	3.3	3756	2026	1469	1730	2287
K52	5	3.9	6203	5069	4490	1135	1713
R42-A0	3	0.2	4	-804	-1312	809	1317
R42-A10	3	0.2	158	-879	-1307	1037	1465
R42-A20	2	1.1	1609	489	-83	1120	1691
R42-A30	1.5	1.0	1918	814	514	1104	1404
R42-A40	1.5	1.0	881	-239	-539	1120	1420
SRA-K0	20	1.6	146	-616	-1111	762	1257
SRA-K32	9	2.0	1143	356	-260	787	1403
SRA-K42	8	2.2	2263	1484	950	779	1313

Note: Positive and negative values indicate material expansion and shrinkage, respectively.

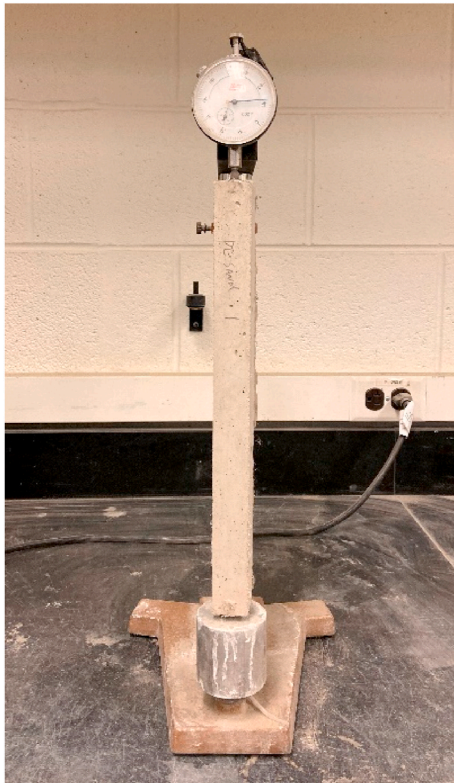


Fig. 2. The setup of the free shrinkage/expansion test.

ring test was developed based on ASTM C1581/C1581M-18a [34]. The difference is that the K42 and SRA-K42 were solid cast inside a steel ring with 405 mm outer diameter and 385 mm inner diameter, rather than a hollow ring in the restrained test [34]. Fig. 3 shows the setup of a steel ring with a height of 150 mm. The expansion of K42 or SRA-K42 applies pressure against the steel ring, and the resulting strain of the steel ring was monitored by 3 strain gauges, starting 5 h after the cast and lasted for 28 d.

According to Shah and Weiss [35], the residual interface pressure between the steel ring and K42/SRA-K42 can be computed by equation (1):

$$p_{residual}(t) = \varepsilon_{steel}(t) E_{steel} \frac{(R_{Osteel}^2 - R_{Isteel}^2)}{2R_{Osteel}^2} \quad (1)$$



Fig. 3. Expansion steel ring test, with three strain gauges attached on the external surface separated by 120° of the steel ring.

where $p_{residual}(t)$ is the residual interface pressure, $\varepsilon_{steel}(t)$ is the strain measured by 3 strain gauges, $E_{steel} = 200$ GPa is Young's modulus of the steel ring given by the manufacturer, $R_{Osteel} = 405$ mm and $R_{Isteel} = 385$ mm are the outer and inner diameter of the steel ring.

2.2.4. Uniaxial tensile test and compressive test

The compressive strengths of the mixtures in Table 3 were determined using $50 \times 50 \times 50$ mm³ cubes. The direct tensile test was performed using a dogbone-shaped specimen as shown in Fig. 4. After 28-day air curing (20 ± 3 °C, $40 \pm 5\%$ RH), 3 cube specimens per mixture were tested in compression following ASTM C109 [36]. 3 dogbone-shaped specimens per mixture were tested on an Instron servo-hydraulic system at a rate of 0.5 mm/min. The deformation was measured by two linear variable displacement transducers (LVDT) with an 80 mm gauge length. During the tensile test, the average crack width (CW) was measured by dividing the tensile elongation by crack number when the dogbone specimen was tensioned to 1%, 2%, and 3% strain levels.

3. Results and discussions

3.1. Drying shrinkage/expansion

3.1.1. Effect of SAP and SRA

Fig. 5 plots the free length change of ECC prisms during air curing (20 ± 2 °C, $40 \pm 5\%$ RH) for 150 d. The drying shrinkage of K0 was -1435 $\mu\epsilon$ at 28 d, which was similar to the drying shrinkage of traditional ECCs (-1200 $\mu\epsilon$ to -1500 $\mu\epsilon$). The shrinkage slowed down after 28 d and reached -2088 $\mu\epsilon$ at 150 d. The drying shrinkage of SAP-K0 and K0 appeared comparable. As drying shrinkage is mainly governed by the water/binder ratio [30,37], SAP showed minimal effect on the reduction of drying shrinkage at the same water/binder ratio. The drying shrinkage of SRA-K0 was -616 $\mu\epsilon$ at 28 d and -1111 $\mu\epsilon$ at 150 d, approximately 50% lower compared to K0 and SAP-K0.

3.1.2. Effect of CSA-K

When part of the OPC was replaced by CSA cement, ECC was found to expand at early age, reaching a maximum value at several hours to a few days, and followed by shrinkage as shown in Fig. 6. The reductions from the maximum expansion to the diminished expansion at 28 and 150 d are defined as the "expansion losses" at 28 and 150 d. Table 4 lists the characteristic expansion of the ECC compositions. Increasing CSA-K content was found to shorten the ECC hardening process but led to a delay in the occurrence of maximum expansion. However, the maximum expansion was increased when a higher amount of CSA-K was introduced. As shown in Fig. 6, despite a large maximum expansion of 779 $\mu\epsilon$ at 2.3 d for K22, the specimen was found to shrink to -832 $\mu\epsilon$ at 28 d and to -1532 $\mu\epsilon$ at 150 d. In contrast, K32 and K42 maintained expansion of 1139 $\mu\epsilon$ and 2026 $\mu\epsilon$ at 28 d, indicating the potential of self-stressing applications. The maximum expansion of K52 (6203 $\mu\epsilon$) exceeded the measured range of the shrinkage instrument at 3.9 d, so data were not collected after that time.

3.1.3. Effect of CSA-R and anhydride

The type of CSA cement also plays a role in the material expansion. At the 42% mass content of the CSA cement (42% substitution of OPC), switching from CSA-K to CSA-R led to a transition from material expansion to material shrinkage at 28 d as observed in Fig. 7. The effect of CSA composition on material length change could be explained by the different SO₃ content in the two CSA cement. Eqs. (2) and (3) show the hydration of ye'elimitite (C₄A₃S̄, the primary mineral phase of CSA cement), ettringite (Eq. (2)) and monosulfoaluminate (Eq. (3)) are formed as the main hydration product besides AH₃ in the gypsum-containing and gypsum-free CSA cement, respectively [38]. As ettringite accounts for the expansive character of CSA-based materials, the

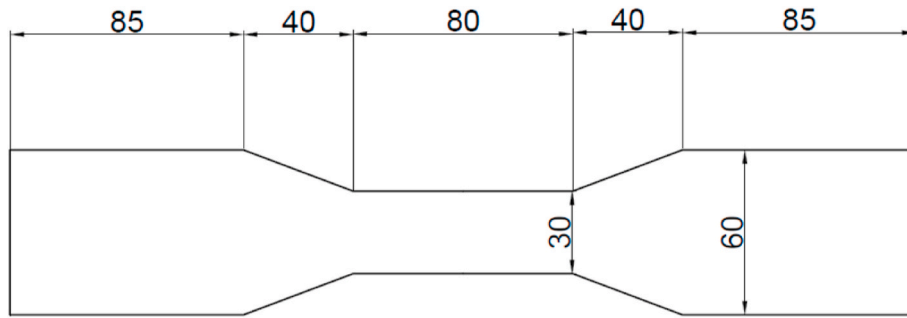


Fig. 4. The dimension of the dogbone-shape specimen. (Unit: mm, thickness 13 mm).

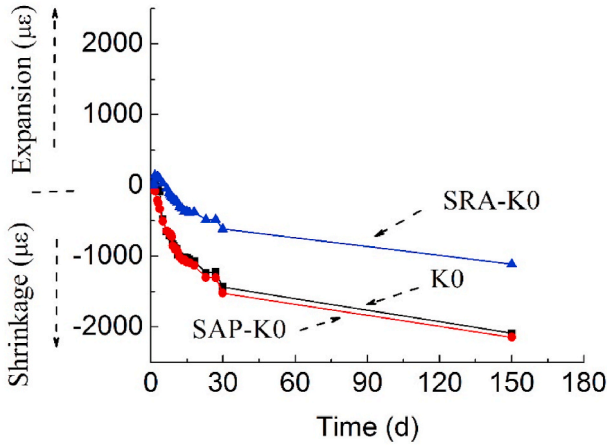


Fig. 5. The effect of SRA and SAP on free expansion/shrinkage of ECC.

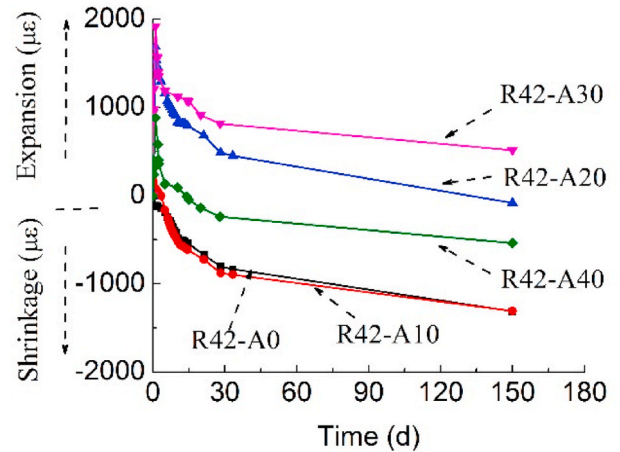


Fig. 7. The free expansion/shrinkage of ECC mixed with CSA-R and anhydride.

By adding anhydride to CSA-R, an increasing material expansion was observed, as shown in Fig. 7. However, there exists an optimal replacement ratio to obtain a maximum expansion. The expansion of R42-A30 was 1918 μϵ (maximum) and 814 μϵ (28 d), however, the maximum expansion of R42-A40 was 881 μϵ and the expansion decreased to -239 μϵ at 28 d. As anhydride must be accompanied by sufficient $C_4A_3\bar{S}$ content to generate expansion [39], the decreasing expansion of R42-A40 was due to the excess substitution of the anhydride, which did not produce ettringite and cause material expansion after $C_4A_3\bar{S}$ was fully depleted.

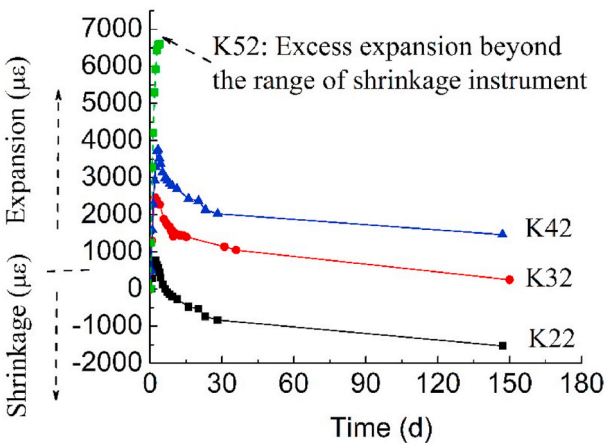
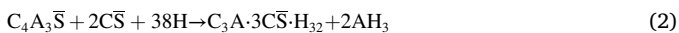


Fig. 6. The free expansion/shrinkage for the ECC composed with CSA-K cement (CSA-K replacement ratios were 22%, 32%, 42%, and 52%).

CSA-K with a relatively higher amount of SO_3 (as shown in Table 1) appeared more effective in promoting ECC expansion as suggested in Fig. 6. This observation agrees with the product instruction provided by the supplier of CSA-R, which was described as a pure CSA clinker with no gypsum or anhydride added. The hydration of CSA-R likely followed Eq. (3) with minimal expansion observed.



where the C, A, \bar{S} , and H denote CaO , Al_2O_3 , SO_3 , and H_2O , respectively.

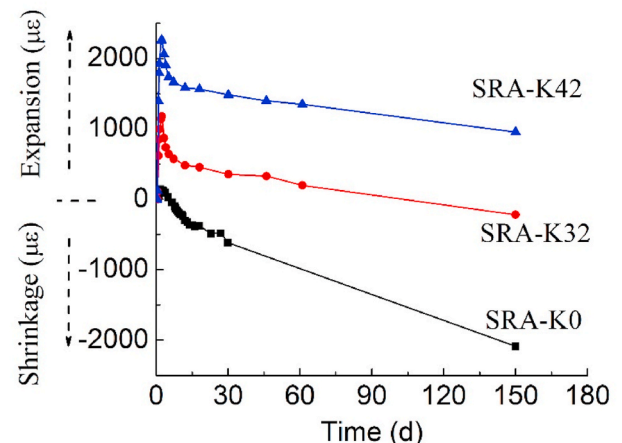


Fig. 8. The effect of combining SRA and CSA-K on free expansion/shrinkage.

3.1.4. Effect of CSA-K and SRA

The expansion results combining SRA and CSA-K are shown in Fig. 8. The maximum expansion of SRA-32 was 1143 $\mu\epsilon$, decreasing to 356 $\mu\epsilon$ at 28 d and $-260 \mu\epsilon$ at 150 d. The SRA-42 had a maximum expansion of 2263 $\mu\epsilon$ at 2.2 d, and retained the expansion of 1484 $\mu\epsilon$ at 28 d and 950 $\mu\epsilon$ at 150 d. Compared with K42, SRA-K42 decreased the maximum expansion from 3756 $\mu\epsilon$ to 2263 $\mu\epsilon$. Additionally, the expansion loss of SRA-K42 was 779 $\mu\epsilon$ at 28 d (55% lower than that of K42) and 1313 $\mu\epsilon$ at 150 d (42% lower than that of K42). Therefore, SRA-K42 reduces the maximum expansion, along with the expansion loss compared with K42. SRA retarded the hydration and produced less ettringite in the hydration product. Additionally, SRA lowered the surface tension of the pore solution [40,41], resulting in the lower expansion loss of SRA-K42.

3.2. Self-stressing ECC

To attain a self-stressing ECC, both the maximum expansion and the subsequent expansion loss should be tailored. A critical maximum expansion was proposed for CSA cement (5000 $\mu\epsilon$) [38], above which the sample itself would experience cracking. The maximum expansion without causing damage depends on the structure geometry and the thickness of repair material. The maximum expansion herein is preferred to be less than 5000 $\mu\epsilon$, which could be further lowered depending on the application. Therefore, the K52 was not desirable for developing the self-stressing ECC due to the excessive amount of expansion.

The volume deformation of CSA and OPC blended cement first expands, followed by a gradual decrease (herein named as expansion loss) [20]. The restrained expansion exerts pressure on the repaired structure. However, the subsequent expansion loss decreases the expansive pressure. Lower expansion loss is desirable for maintaining expansive pressure. Assuming linear material constitutive behavior, the pressure caused by the repair material expansion can be expressed as:

$$p = E_1 \varepsilon_1 - E_2 \varepsilon_2 \quad (4)$$

where p is the pressure exerted by the expansive ECC; ε_1 is the maximum expansion of ECC; ε_2 is the expansion loss; E_1 is the effective modulus between zero time and maximum expansion time; E_2 is the effective modulus of ECC between maximum expansion time and 28/150 d ε_1 and ε_2 are listed in Table 4. E_1 and E_2 are influenced by stress relaxation and time development. ECC has lower elastic modulus and prominent creep property at an early age (before 3 d) but attains a higher elastic modulus and negligible creep property at a later age (3–28 days) [20,24]. Thus, though the final volume deformation appears expansive, tensile stress may form in the final ECC posing a risk of material cracking if the second

term in (4) overwhelms the first term.

Assuming that $E_1 = kE_2$, the pressure can also be expressed as:

$$f = (k\varepsilon_1 - \varepsilon_2)E_2 \quad (5)$$

where k is defined as the coefficient of effective modulus. k is determined by the combined effect of material elastic modulus development and boundary restraint condition. To ensure the self-stressing effect, $(k\varepsilon_1 - \varepsilon_2)$ should be larger than 0.

According to Refs. [24,42,43], it seems plausible to assume that k is between 0.4 and 0.5. In other words, the expansion loss is preferred to be lower than 60% of the maximum expansion to obtain a self-stressing effect. Though some mixtures in Table 4 show expansion at 28/150 d, only K42 and SRA-K42 had the ratio of expansion loss to maximum expansion smaller than 50%–60%. The expansion loss to the maximum expansion ratio of K42 was 46% at 28 d and 61% at 150 d. SRA-K42 showed a lower ratio of 34% at 28 d and 58% at 150 d.

An expansive steel ring test was performed for K42 and SRA-K42 to verify their self-stressing ability as discussed above. Fig. 9 plots the measured expansion of the steel ring and the corresponding interface pressure calculated by Eq. (1). Similar to free expansion results in Table 4, SRA-K42 reduced the maximum expansion compared to K42. Meanwhile, the expansion loss of SRA-K42 was smaller than that of K42. Fig. 9 (b) indicates that the interface pressure of SRA-K42 maintained a relatively stable value due to its lower shrinkage, while the interface pressure of K42 continually decreased to approximately 0 MPa. Though the expansion loss of K42 made up only 46% of the maximum expansion at 28d, the expansive pressure was counteracted due to the larger elastic modulus and less stress relaxation at later age. SRA-K42 retained 0.4 MPa expansive stress at 28 d to attain the self-stress effect.

3.3. Mechanical performance of the self-stressing ECC

Fig. 10 depicts the tensile stress-strain relationships of K0, SRA-K0, K42, and SRA-K42. Table 5 lists the compressive strength and the tensile properties (ultimate tensile strength, strain capacity, crack width and crack spacing) of the self-stressing ECC (SRA-K42). Compared to K0, the compressive strength and ultimate tensile strength of K42 increased from 30 MPa to 32 MPa and from 3.4 MPa to 3.9 MPa, respectively. The tensile strain capacity of K42 was 5% higher than that of K0 (3.7%). The expanded ettringite produced by CSA cement enhanced the interfacial bonding of PP-Matrix [27] and induced a higher fiber bridging stress, contributing to the higher ultimate tensile strength and ductility than K0.

Compared with K0 and K42, the addition of SRA decreased the compressive strength by 12%–13% and the ultimate tensile strength by

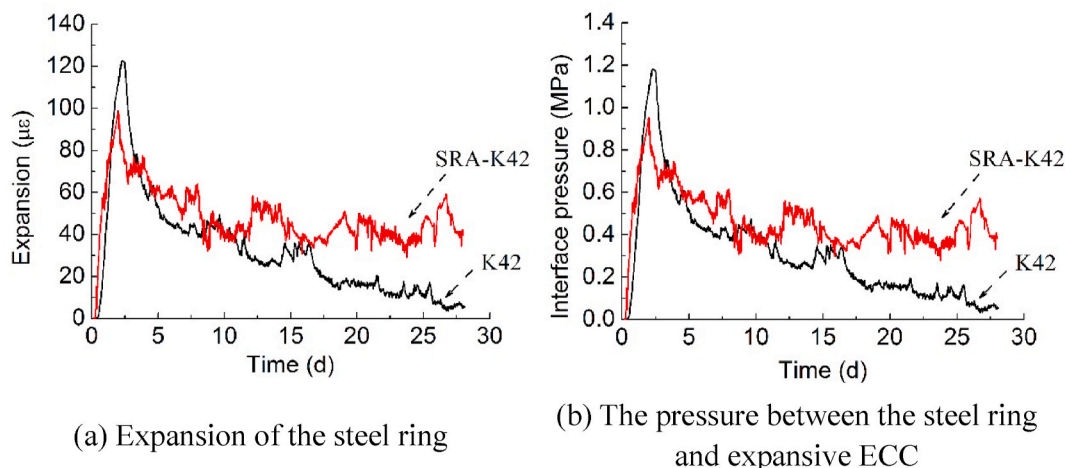


Fig. 9. The measured expansion and computed expansive pressure of the steel ring test.

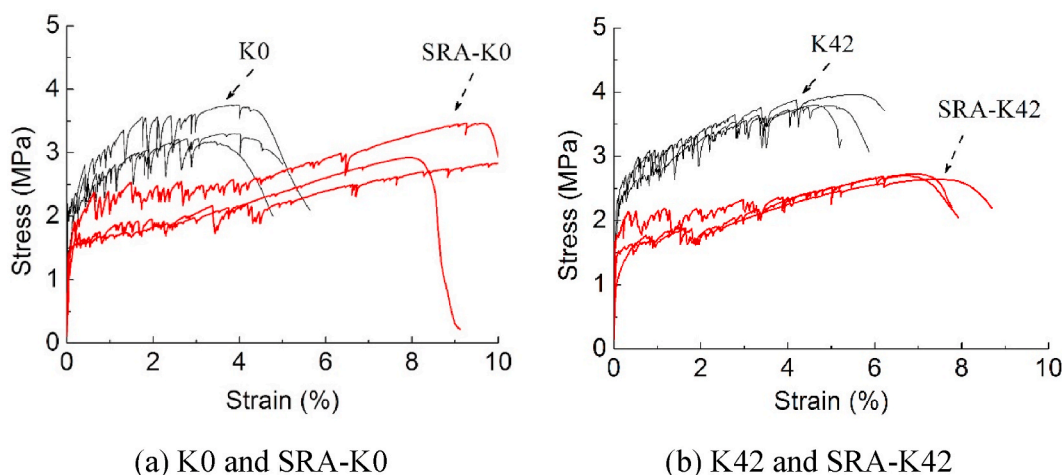


Fig. 10. Tensile stress-strain relationships of ECC.

Table 5

Compressive strength and tensile properties of composites at 28 d.

Mixture	f_c (MPa)	f_t (MPa)	ε_t ($\mu\epsilon$)	Crack width (μm)			Crack spacing (mm)		
				1%	2%	3%	1%	2%	3%
K0	30.0 ± 1.5	3.4 ± 0.3	3.7 ± 0.3	85 ± 8	109 ± 2	114 ± 8	8.5	5.4	3.8
SRA-K0	25.9 ± 2.3	2.8 ± 0.1	9.2 ± 1.2	42 ± 13	46 ± 11	54 ± 14	4.2	2.3	1.8
K42	32.1 ± 1.5	3.9 ± 0.1	5.0 ± 0.4	61 ± 4	82 ± 8	99 ± 10	6.1	4.1	3.3
SRA-K42	28.2 ± 1.6	2.7 ± 0.1	7.0 ± 0.3	35 ± 3	38 ± 1	44 ± 1	3.5	1.9	1.5

Note: f_c , f_t , and ε_t denote compressive strength, ultimate tensile strength, and tensile strain capacity, respectively.

17–31%. SRA delays the cement setting, resulting in changes in formation and uniform distribution of calcium-silicate-hydrate (C–S–H) gels [44]. SRA increases the total porosity and the pores larger than $0.1 \mu\text{m}$ [40], leading to the reduction of strength. SRA addition significantly increased the tensile strain capacity as observed in Table 5 and Fig. 10. The average tensile strain capacity of SRA-K0 and SRA-K42 was 9% and 7%, much higher than that of the PP reinforced ECC composite in the literature (1.0%–3.9%) [4,45,46]. PP fiber reduces approximately 50% of the fiber cost when compared with Polyvinyl Alcohol (PVA) fiber [49]. However, the tensile strength of PP fiber (850 MPa) makes up only 53% of PVA fiber (1600 MPa) [29], which may hinder the mechanical performance of PP reinforced ECC. Despite the lower strength of PP fiber, the ultra-high tensile strain capacity of SRA-K42 shows an advantage over conventional PVA-M45-ECC with a 3.7% strain capacity [29]. Though SRA impeded the strength development, the compressive strength of 28 MPa and the ultimate tensile strength of 2.7 MPa is adequate for most normal repair cementitious materials [50]. For the repair of infrastructures such as bridge, tunnel, and pavement, deformation capacity is more important than higher strength capacity. Cracks are mainly caused by uneven or imposed deformation other than overload [6,47]. SRA increased the ductility and decreased the shrinkage of ECC, leading to SRA-K42 competitive in concrete/cement applications.

The relatively large crack width is one of the main challenges for PP-ECC when compared with PVA-ECC. The crack width of K0 below 3% was 85–114 μm , consistent with the reported crack width (95–151 μm) in Refs. [4,46]. Partially replacing OPC with CSA (K42) decreased the average crack width to 61–99 μm , which could be attributed to the enhanced frictional bond due to the expansive force of the matrix against the fiber [27]. SRA addition further reduced the crack width to 35–44 μm at tensile strains below 3%, which was smaller than that of typical PVA-ECC (50–80 μm) [5]. SRA reduces shrinkage and effectively further increases the expansive force of the matrix against the fiber, translating into a tighter grip on the fiber that resists cracking opening. The tight crack spacing (dividing the gauge length by the crack number

while tensioning) of SRA-K42 listed in Table 5 and the crack patterns shown in Fig. 11 demonstrated the tight crack and ultra-high tensile strain capacity of the self-stressing ECC (SRA-K42).

4. Conclusions

Based on the above findings, a self-stressing ECC with ultra-high ductility was developed by combining the use of calcium sulphoaluminate (CSA) expansive additive/cement and shrinkage reducing agent (SRA). Specifically, the following conclusions can be drawn:

- The level of expansion of ECC blended with CSA and OPC depends on the CSA content and type. When OPC is partially replaced by 42% CSA with high sulfate content (CSA-K), the composite attains an expansion of 2026 μe at 28 days; the same replacement but using CSA with low sulfate content (CSA-R), however, leads to shrinkage of $-804 \mu\text{e}$ at 28 days.
- The addition of anhydrite to CSA-R up to 30% was found to increase the expansion, but diminish the expansion with further addition.
- The initial CSA-OPC-ECC expansion is followed by an expansion loss after reaching a peak at a few hours to a few days. The expansive pressure induced on restraint (such as a steel ring) is influenced by the time-dependent expansion deformation as well as the elastic modulus and creep development with age. The self-stressing effect is achieved by limiting the expansion loss. The addition of SRA lowers the capillary surface tension and reduces the expansion loss, leading to a self-stressing ECC of SRA-K42.
- Introducing CSA in ECC increases the tensile strength and ductility, while SRA addition decreases the strength. The combination of CSA-K and SRA attains an ECC with ultra-high tensile strain capacity up to 7%, and the average crack width of 35–44 μm at tensile strains less than 3%. Despite the lower strength due to SRA addition, the ultra-high tensile strain capacity, tight multiple-cracking, as well as the

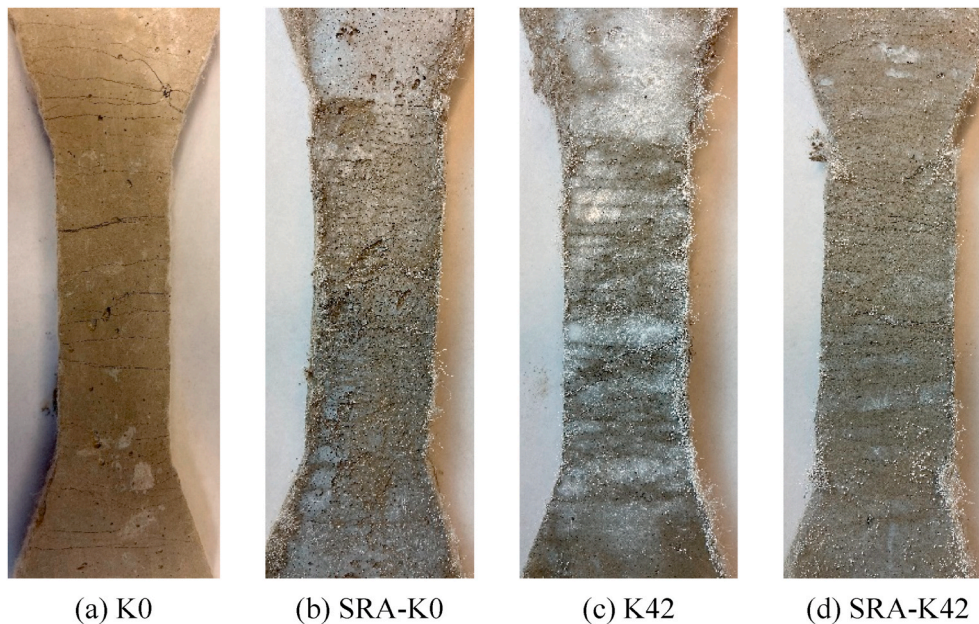


Fig. 11. Crack patterns of ECCs under uniaxial tension.

self-stressing effect promotes the use of SRA-K42 ECC as a promising repair material for concrete infrastructure.

Declaration of competing interest

The authors declare that they have no known competing financial interests or personal relationships that could have appeared to influence the work reported in this paper.

Acknowledgments

This research is partially supported by the Center for Low Carbon Built Environment at the University of Michigan. Materials supply from BORAL RESOURCES (fly ash), CTS Cement Manufacturing Corp. (CSA-K), USG Corporation (Anhydrite), BASF (water reducer), Sanyo Corporation (SAP), GCP applied technologies (SRA) is gratefully acknowledged.

References

- [1] ASCE, Infrastructure Report Card, ASCE Reston, VA, 2017.
- [2] Y. Yang, Y. Yao, X. Gao, H. Deng, P. Yu, Shrinkage reducing measures for engineering cementitious composites, *J. Wuhan Univ. Technol.-Materials Sci. Ed.* 23 (2008) 907–911.
- [3] H. Zhu, Y. Hu, Q. Li, R. Ma, Restrained cracking failure behavior of concrete due to temperature and shrinkage, *Construct. Build. Mater.* 244 (2020), 118318.
- [4] Q. Zhang, V.C. Li, Development of durable spray-applied fire-resistive engineered cementitious composites (SFR-ECC), *Cement Concr. Compos.* 60 (2015) 10–16.
- [5] V.C. Li, *Engineered Cementitious Composites (ECC): Bendable Concrete for Sustainable and Resilient Infrastructure*, Springer, 2019.
- [6] Y.Y. Kim, G. Fischer, Y.M. Lim, V.C. Li, Mechanical performance of sprayed engineered cementitious composite using wet-mix shotcreting process for repair applications, *ACI Mater. J.* 101 (2004) 42–49.
- [7] J. Zhang, C. Gong, Z. Guo, M. Zhang, Engineered cementitious composite with characteristic of low drying shrinkage, *Cement Concr. Res.* 39 (2009) 303–312.
- [8] M.B. Weimann, V.C. Li, Drying Shrinkage and Crack Width of Engineered Cementitious Composites (ECC), in: *Brittle Matrix Composites*, vol. 7, Woodhead Publishing, 2003, pp. 37–46.
- [9] X. Kong, Z. Zhang, Z. Lu, Effect of pre-soaked superabsorbent polymer on shrinkage of high-strength concrete, *Mater. Struct.* 48 (2015) 2741–2758.
- [10] Y. Yao, Y. Zhu, Y. Yang, Incorporation superabsorbent polymer (SAP) particles as controlling pre-existing flaws to improve the performance of engineered cementitious composites (ECC), *Construct. Build. Mater.* 28 (2012) 139–145.
- [11] X. Ma, J. Liu, Z. Wu, C. Shi, Effects of SAP on the properties and pore structure of high performance cement-based materials, *Construct. Build. Mater.* 131 (2017) 476–484.
- [12] Q. Ran, N. Gao, J. Liu, Q. Tian, J. Zhang, Shrinkage action mechanism of shrinkage-reducing admixtures based on the pore solution, *Mag. Concr. Res.* 65 (2013) 1092–1100.
- [13] S. Gao, Z. Wang, W. Wang, H. Qiu, Effect of shrinkage-reducing admixture and expansive agent on mechanical properties and drying shrinkage of Engineered Cementitious Composite (ECC), *Construct. Build. Mater.* 179 (2018) 172–185.
- [14] A.N. Lopes, E.F. Silva, D.C. Dal Molin, R.D. Toledo Filho, Shrinkage-reducing admixture: effects on durability of high-strength concrete, *ACI Mater. J.* 110 (2013) 365.
- [15] J. Wang, N. Banthia, M. Zhang, Effect of shrinkage reducing admixture on flexural behaviors of fiber reinforced cementitious composites, *Cement Concr. Compos.* 34 (2012) 443–450.
- [16] J. Zhang, C. Gong, Z. Guo, M. Zhang, Engineered cementitious composite with characteristic of low drying shrinkage, *Cement Concr. Res.* 39 (2009) 303–312.
- [17] R. Trauchessec, J. Mechling, A. Lecomte, A. Roux, B. Le Rolland, Impact of anhydrite proportion in a calcium sulfoaluminate cement and Portland cement blend, *Adv. Cement Res.* 26 (2014) 325–333.
- [18] L. Pelletier, F. Winnefeld, B. Lothenbach, The ternary system Portland cement–calcium sulfoaluminate clinker–anhydrite: hydration mechanism and mortar properties, *Cement Concr. Compos.* 32 (2010) 497–507.
- [19] J. Han, D. Jia, P. Yan, Understanding the shrinkage compensating ability of type K expansive agent in concrete, *Construct. Build. Mater.* 116 (2016) 36–44.
- [20] W. Choi, H. Yun, Effect of expansive admixtures on the shrinkage and mechanical properties of high-performance fiber-reinforced cement composites, *Sci. World J.* (2013) 2013.
- [21] S. Shadravan, C. Ramseyer, T.H.K. Kang, A long term restrained shrinkage study of concrete slabs on ground, *Eng. Struct.* 102 (2015) 258–265.
- [22] M.S. Meddah, M. Suzuki, R. Sato, Influence of a combination of expansive and shrinkage-reducing admixture on autogenous deformation and self-stress of silica fume high-performance concrete, *Construct. Build. Mater.* 25 (2011) 239–250.
- [23] Y. Lu, Z. Liu, S. Li, W. Li, Behavior of steel fibers reinforced self-stressing and self-compacting concrete-filled steel tube subjected to bending, *Construct. Build. Mater.* 156 (2017) 639–651.
- [24] H. Zhu, Q. Li, Y. Hu, R. Ma, Double feedback control method for determining early-age restrained creep of concrete using a temperature stress testing machine, *Materials* 11 (2018) 1079.
- [25] H. Shuguang, L. Yue, Research on the hydration, hardening mechanism, and microstructure of high performance expansive concrete, *Cement Concr. Res.* 29 (1999) 1013–1017.
- [26] R. Sahamitmongkol, T. Kishi, Tensile behavior of restrained expansive mortar and concrete, *Cement Concr. Compos.* 33 (2011) 131–141.
- [27] R.B. Jewell, K.C.M. Thomas, Interfacial bond between reinforcing fibers and calcium sulfoaluminate cements: fiber pullout characteristics, *ACI Mater. J.* 112 (2015) 39–48.
- [28] M. Li, V.C. Li, Rheology, fiber dispersion, and robust properties of Engineered Cementitious Composites, *Mater. Struct.* 46 (2013) 405–420.
- [29] H. Wu, D. Zhang, Y. Du, V.C. Li, Durability of engineered cementitious composite exposed to acid mine drainage, *Cement Concr. Compos.* 108 (2020), 103550.
- [30] X. Kong, Z. Zhang, Z. Lu, Effect of pre-soaked superabsorbent polymer on shrinkage of high-strength concrete, *Mater. Struct.* 48 (2015) 2741–2758.
- [31] Q. Ran, N. Gao, J. Liu, Q. Tian, J. Zhang, Shrinkage action mechanism of shrinkage-reducing admixtures based on the pore solution, *Mag. Concr. Res.* 65 (2013) 1092–1100.

- [32] D. Yoo, N. Banthia, Y. Yoon, Effectiveness of shrinkage-reducing admixture in reducing autogenous shrinkage stress of ultra-high-performance fiber-reinforced concrete, *Cement Concr. Compos.* 64 (2015) 27–36.
- [33] ASTM C490/C490M-17, Standard Practice for Use of Apparatus for the Determination of Length Change of Hardened Cement Paste, Mortar, and Concrete, ASTM International, West Conshohocken, PA, 2017.
- [34] ASTM C1581/C1581M-18a, Standard Test Method for Determining Age at Cracking and Induced Tensile Stress Characteristics of Mortar and Concrete under Restrained Shrinkage, ASTM International, West Conshohocken, PA, 2018.
- [35] H.R. Shah, J. Weiss, Quantifying shrinkage cracking in fiber reinforced concrete using the ring test, *Mater. Struct.* 39 (2006) 887.
- [36] ASTM C109/C109M-20a, Standard Test Method for Compressive Strength of Hydraulic Cement Mortars (Using 2-in. Or [50-mm] Cube Specimens), ASTM International, West Conshohocken, PA, 2020.
- [37] X. Ma, J. Liu, Z. Wu, C. Shi, Effects of SAP on the properties and pore structure of high performance cement-based materials, *Construct. Build. Mater.* 131 (2017) 476–484.
- [38] J. Bizzozero, C. Gosselin, K.L. Scrivener, Expansion mechanisms in calcium aluminate and sulfoaluminate systems with calcium sulfate, *Cement Concr. Res.* 56 (2014) 190–202.
- [39] I.A. Chen, C.W. Hargis, M.C.G. Juenger, Understanding expansion in calcium sulfoaluminate–belite cements, *Cement Concr. Res.* 42 (2012) 51–60.
- [40] S. Gao, Z. Wang, W. Wang, H. Qiu, Effect of shrinkage-reducing admixture and expansive agent on mechanical properties and drying shrinkage of Engineered Cementitious Composite (ECC), *Construct. Build. Mater.* 179 (2018) 172–185.
- [41] V. Corinaldesi, Combined effect of expansive, shrinkage reducing and hydrophobic admixtures for durable self compacting concrete, *Construct. Build. Mater.* 36 (2012) 758–764.
- [42] S.A. Altoubat, D.A. Lange, Creep, shrinkage, and cracking of restrained concrete at early age, *ACI Mater. J.* 98 (2001) 323–331.
- [43] Y. Wei, W. Hansen, Tensile creep behavior of concrete subject to constant restraint at very early ages, *J. Mater. Civ. Eng.* 25 (2013) 1277–1284.
- [44] O. Demir, Ö. Sevim, E. Tekin, The effects of shrinkage-reducing admixtures used in self-compacting concrete on its strength and durability, *Construct. Build. Mater.* 172 (2018) 153–165.
- [45] E. Yang, V.C. Li, Strain-hardening fiber cement optimization and component tailoring by means of a micromechanical model, *Construct. Build. Mater.* 24 (2010) 130–139.
- [46] B. Felekoglu, K. Tosun-Felekoglu, R. Ranade, Q. Zhang, V.C. Li, Influence of matrix flowability, fiber mixing procedure, and curing conditions on the mechanical performance of HTPP-ECC, *Compos. B Eng.* 60 (2014) 359–370.
- [47] H. Zhu, Q. Li, R. Ma, L. Yang, Y. Hu, J. Zhang, Water-repellent additive that increases concrete cracking resistance in dry curing environments, *Construct. Build. Mater.* 249 (2020), 118704.
- [48] ASTM C403/C403M-16, Standard Test Method for Time of Setting of Concrete Mixtures by Penetration Resistance, ASTM International, West Conshohocken, PA, 2016.
- [49] H. Zhu, Z. Duo, T. Wang, H. Wu, V.C. Li, Mechanical and self-healing behavior of low carbon engineered cementitious composites reinforced with PP-fibers, *Construct. Build. Mater.* 259 (2020), 119805.
- [50] H. Zhu, K. Yu, V.C. Li, Sprayable engineered cementitious composites (ECC) using calcined clay limestone cement (LC3) and PP fiber, *Cement Concr. Compos.* 115 (2021), 103868.